PERIODIC NONLINEAR CIRCUITS

The steady-state analyses of nonlinear circuits are very important in the design of communication circuits such as amplifiers, oscillators, modulators, and so on. In the case of a linear circuit driven by a periodic sinusoidal source, the circuit will eventually exhibit a *periodic steady-state* response as a particular solution of the ordinary differential equation. However, when the circuit is nonlinear and driven by a sinusoidal input, the steady-state waveform will contain many higher harmonic components depending on the nonlinearities. For the example of an RC amplifier, the circuit will behave like a linear circuit for small sinusoidal input. When the input is increased, however, many higher harmonic components will be contained in the output waveform because of the strong nonlinearity. It is also known that the distortion of an oscillator mainly depends on the choice of the dc operating point.

Input signals of communication circuits usually contain multiple frequency components, and modulators and mixers are driven by multiple inputs whose output also contains many frequencies by the linear combinations of the input signals. In these cases, if the input frequencies are related in irrationally, the response is called a *quasi-periodic* solution and does not have any period. Consider an amplitude modulator with two inputs, one of which is a high-frequency carrier signal and the other a low-frequency input signal. Then, the modulated response will behave as a quasi-periodic function whose frequency spectrum is concentrated in the vicinity of the carrier frequency.

Although the steady-state responses can be calculated by the *brute-force* numerical integration technique (1), it requires considerable computation time (especially in weakly damped circuits) since the transient term dies very slowly. There are two basic approaches for calculating the periodic steady-state responses, namely, the *time-domain approach* (2–8) and the *frequency-domain approach* (9–12). The former is based on the transient analysis, where the initial guess giving rise to the *periodic* steady-state response is first determined by the Newton method (2–5), whose Jacobian matrix is estimated by transient analyses of the sensitivity circuit. In this approach, the computational efficiency rapidly decreases for circuits having many state variables, which correspond to the inductor currents and capacitor voltages. Fortunately, in many practical circuits, some of the variables in the sensitivity analyses are damped so fast that we can neglect the effects without further computation (5). Extrapolation (6), which predicts the initial guess from the sampled data of the periodic points in the transient, is a very simple algorithm, and has large convergence ratios for some kinds of circuits.

The computer algorithms (13,14) for calculating the quasi-periodic steady-state responses are much more complicated when compared with those for finding periodic responses. The former (13) finds the initial guess by the Newton method, and the latter (14) is based on the Poincaré map on the phase plane. An amplitude modulator having a large carrier and a sufficiently small signal can be calculated in two steps (15); namely, first the response to the carrier is calculated by a time-domain Newton method, and then that to the small signal can be calculated by solving the time-varying linear sensitivity circuit in the frequency domain. This method can also be applied to noise analysis (16). Since all of the time-domain methods are based on the transient analyses, they can be efficiently applied to circuits containing any kind of nonlinear elements. In order to calculate the Jacobian matrix, we need to solve the sensitivity circuit starting from different unit initial conditions, equal to the number of state variables. Therefore, this is rather time-consuming for large scale circuits containing many inductors and capacitors.

In the *frequency-domain* approach, the steady-state solutions are described by trigonometric-series representations, and their coefficients are calculated by the method of balancing the responses between the linear and nonlinear subcircuits. For a linear circuit, the response can be easily calculated by exploiting both the superposition theorem and the phasor technique. However, in nonlinear circuits, the calculation of the trigonometric-series coefficients is difficult compared to the linear circuits, because superposition can no longer be applied. There are two basic methods based on the *harmonic balance method* (9,10,17,18), and the *relaxation method* (19,20). The harmonic balance method is efficient when the number of nonlinear elements is relatively a few and the nonlinearities are not strong. For example, if we assume the steady-state waveform contains a dc component and M frequency components for N nonlinear elements, there exist $N(2M + 1)$ trigonometric coefficients to be determined. The *determining equation* can be solved by the Newton method (9,10) and/or the modified method (11). In particular, the waveforms of circuits driven by multitone signals may have many frequency components resulting from linear combinations of the input frequency components. Hence, when the nonlinearities are strong, we must solve a system of large determining equations even for small circuits (21,22).

Conversely, *relaxation methods* (19,23) are very simple algorithms and are efficiently applied to large scale circuits if they are partitioned into the linear subnetworks and the small scale nonlinear subnetworks, where the variational values at each iteration can be calculated by the time-invariant sensitive linear circuit. Although the algorithm is used for weakly nonlinear circuits, it can be also efficiently applied to the stiff circuits containing transistors and diodes if we introduce a compensatory technique (19) for weakening the nonlinearity.

At this point, we can conclude that the *time-domain methods* may be efficiently applied to small-scale circuits containing strong nonlinear elements. On the other hand, the *fre-*

quency-domain methods are useful for weakly nonlinear circuits having few nonlinear elements.

Usually, large scale communication systems are composed of many subsystems such as modulators, filters, and so on, some of which may be classified into linear and nonlinear subcircuits. Therefore, we recommend partitioning a given large system into small-scale subcircuits and applying an appropriate algorithm to each subcircuit. The relaxation hybrid harmonic balance method consists of different kinds of algorithms, where the linear and/or weakly nonlinear subcircuits are solved by a frequency-domain approach and the strong nonlinear subcircuits are solved by a time-domain approach (20,23). Therefore, the large scale circuits can be efficiently solved by the application of the circuit partitioning technique and the relaxation hybrid harmonic balance method.

TIME-DOMAIN APPROACH

The transient responses of nonlinear circuits are *uniquely* decided once the initial guess $\mathbf{x}(0)$ of the state-variables is given. Therefore, the steady-state response can be found if we can find the solution satisfying $\mathbf{x}(0) - \mathbf{x}(T) = \mathbf{0}$. The equation is efficiently solved by the Newton and extrapolation methods.

Forced Circuits

In the computer-aided analysis of nonlinear circuits with periodic inputs, the steady-state periodic response is found by simply integrating the system equation from a given initial point until the response becomes periodic, which is called a *brute-force* method. In lightly damped systems, however, the method requires much more computation time. In this section, the Newton algorithm (2) is shown which converges rapidly to the steady state.

Consider a set of the system equations

$$\mathbf{f}(\dot{\mathbf{x}}, \mathbf{x}, \mathbf{y}, \omega t) = \mathbf{0}, \quad \mathbf{f}(\cdot): \mathbb{R}^{n+m+1} \to \mathbb{R}^{n+m} \tag{1}$$

where $x \in \mathbb{R}^n$ is the state variable vector, $y \in \mathbb{R}^m$ the nonstate variable vector. Then, the steady-state solution satisfies the following *determining equation:*

$$\mathbf{F}(\mathbf{x}(0)) = \mathbf{x}(0) - \mathbf{x}(T) = \mathbf{0} \tag{2}$$

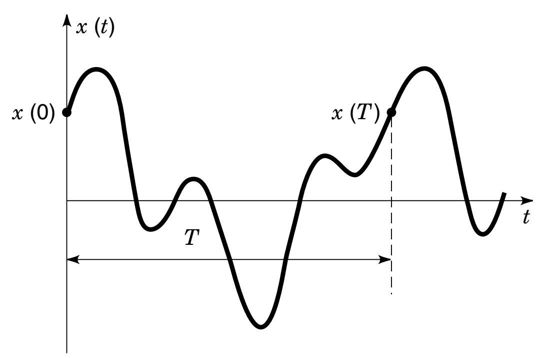

Figure 1. Schematic diagram of steady-state periodic solution.

The schematic diagram is given in Fig. 1, where T denotes the period. Now, apply the Newton method to Eq. (2).

$$\mathbf{x}^{j+1}(0) = \mathbf{x}^{j}(0) = \left[\left. \frac{\partial \mathbf{F}(\mathbf{x}(0))}{\partial \mathbf{x}(0)} \right|_{\mathbf{x}(0)=\mathbf{x}^{j}(0)} \right]^{-1} \mathbf{F}(\mathbf{x}^{j}(0)) \tag{3}$$

The Jacobian matrix of Eq. (2) is given by

$$\frac{\partial \mathbf{F}(\mathbf{x}(0))}{\partial \mathbf{x}(0)} = \mathbf{1} - \frac{\partial \mathbf{x}(T)}{\partial \mathbf{x}(0)} \tag{4}$$

Let $(\mathbf{x}^j(t), \mathbf{y}^j(t))$ be the solution at the jth iteration of Eq. (3). To obtain the variational equation, set

$$\mathbf{x}(t) = \mathbf{x}^{j}(t) + \eta(t), \quad \mathbf{y}(t) = \mathbf{y}^{j}(t) + \delta(t) \tag{5}$$

Then, we have from Eq. (1)

$$\mathbf{f}(\dot{\mathbf{x}}^{j}, \mathbf{x}^{j}, \mathbf{y}^{j}, \omega t) + \left[\frac{\partial \mathbf{f}}{\partial \dot{\mathbf{x}}} \; \frac{\partial \mathbf{f}}{\partial \mathbf{x}} \; \frac{\partial \mathbf{f}}{\partial \mathbf{y}} \right] \Bigg|_{\substack{x=x^j \\ y=y^j}} \begin{bmatrix} \dot{\eta}(t) \\ \eta(t) \\ \delta(t) \end{bmatrix} = \mathbf{0} \tag{6}$$

where it is assumed that $f(\dot{x}^j, x^j, y^j, \omega t) = 0$. Thus, we have

$$\begin{bmatrix} \dot{\eta}(t) \\ \delta(t) \end{bmatrix} = - \left[\frac{\delta \mathbf{f}}{\partial \dot{\mathbf{x}}} \; \frac{\partial \mathbf{f}}{\partial \mathbf{y}} \right]^{-1} \Bigg|_{\substack{x=x^j \\ y=y^j}} \frac{\partial \mathbf{f}}{\partial \mathbf{x}} \eta(t) \tag{7}$$

We rewrite the first row of Eq. (7) into the following form:

$$\dot{\eta}(t) = \mathbf{A}(t)\eta(t) \tag{8}$$

Equation (8) is the linear time-varying system corresponding to the *sensitivity circuit.* Let the *fundamental matrix solution* be $\mathbf{\Phi}(t)$. Then, we have from Eq. (8)

$$\eta(t) = \mathbf{\Phi}(t)\eta(0) \tag{9}$$

which corresponds to

$$\frac{\partial \mathbf{x}(T)}{\partial \mathbf{x}(0)} = \mathbf{\Phi}(T) \tag{10}$$

In practice, the fundamental matrix solution $\mathbf{\Phi}(T)$ can be obtained by solving the time-varying sensitivity circuit from n different unit initial values for the state-variables.

Example

Now, we show the efficiency of the shooting method for the RC-amplifier shown in Fig. 2(a). A comparison between the brute-force method and the shooting method are shown in Fig. 2(b), where the transistor is modeled by the Ebers-Moll model (24). We can calculate the steady-state response with five iterations, where the error is defined by

$$\epsilon^{j} = \sqrt{(v_1^j(0) - v_1^j(T))^2 + (v_2^j(0) - v_2^j(T))^2 + (v_3^j(0) - v_3^j(T))^2}$$

Oscillator Circuits

The steady-state periodic oscillation of an autonomous system is usually calculated by the numerical integration technique (1) from an initial state, which is also time-consuming for

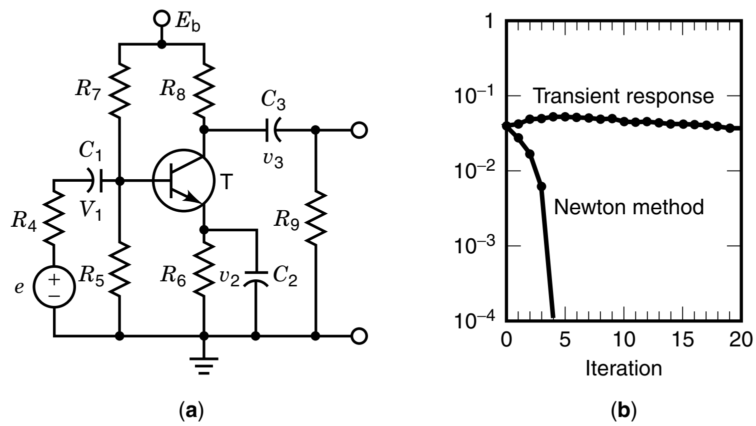

Figure 2. Steady-state response of the RC amplifier (a); C_1 = 10 μF, C_2 = 50 μF, C_3 = 10 μF, R_4 = 2.2 kΩ, R_5 = 12 kΩ; R_6 = 1 kΩ, R_7 = 56 kΩ, R_8 = 10 kΩ, R_9 = 1 kΩ, E_b = 20 V; $e(t)$ = 0.1 sin $10^4 t$. (b) Convergence ratio.

lightly damped oscillators. Furthermore, there are many kinds of coupled oscillators which have many modes oscillation (25), some of which may be stable and others unstable. In this case, the orbits of unstable oscillations can never be found by the numerical integration techniques. Now, we show the time-domain shooting method for autonomous systems that can be used to calculate both the *stable* and *unstable* oscillations once the appropriate initial guesses are given. Consider a system equation

$$\mathbf{f}(\dot{\mathbf{x}}, \mathbf{x}, \mathbf{y}) = \mathbf{0}, \quad \mathbf{f}(\cdot) : \mathbb{R}^{n+m} \rightarrow \mathbb{R}^{n+m} \tag{11}$$

where $\mathbf{x}$ is the state variable vector and $\mathbf{y}$ the non-state variable vector. The period T is considered as a variable. It is defined by the time difference between one of the state variables x_k passing through the same value x_{k0} in the transient response as shown in Fig. 3.

Thus, the steady-state response satisfies the following *determining equation:*

$$\mathbf{F}(\mathbf{x}(0), T) = \mathbf{x}(0) - \mathbf{x}(T) = \mathbf{0} \tag{12}$$

Observe that since $x_k = x_{k0}$ is fixed, the variables are given by

$$\{x_1(0), \ldots, x_{k-1}(0), x_{k+1}(0), \ldots, x_n(0)\} \tag{13}$$

The determining equation can also be solved by the Newton method (3,4). We show an application of the algorithm for a sample example of van der Pol oscillator.

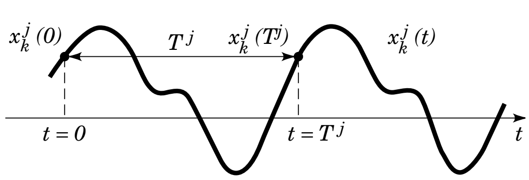

Figure 3. A definition T of an autonomous system.

Example

Consider an oscillator with a tunnel diode as shown in Fig. 4. The system equation is given by

$$f(v_C + E) + Gv_C + \frac{dv_C}{dt} + i_L = 0 \tag{14a}$$

$$L\frac{di_L}{dt} - v_C = 0 \tag{14b}$$

where

$$f(v_C + E) = -\rho_1 v_C + \rho_3 v_C^3 + I_0, \quad \rho_1,\ \rho_3 > 0$$

The determining equation for calculating the steady-state oscillation is given by

$$\begin{bmatrix} F_1(v_C(0), T) \\ F_2(v_C(0), T) \end{bmatrix} = \begin{bmatrix} v_C(0) \\ i_L(0) \end{bmatrix} - \begin{bmatrix} v_C(T) \\ i_L(T) \end{bmatrix} = \mathbf{0} \tag{15}$$

Now, let us calculate the Jacobian matrix for the variables $(v_c(0), T)$

$$\left.\begin{bmatrix} \dfrac{\partial F_1}{\partial v_C(0)} & \dfrac{\partial F_1}{\partial t} \\ \dfrac{\partial F_2}{\partial v_C(0)} & \dfrac{\partial F_2}{\partial t} \end{bmatrix}\right|_{t=T} = \left.\begin{bmatrix} 1 - \dfrac{\partial v_C(t)}{\partial v_C(0)} & -\dfrac{\partial v_C(t)}{\partial t} \\ -\dfrac{\partial i_L(t)}{\partial v_C(0)} & -\dfrac{\partial i_L(t)}{\partial t} \end{bmatrix}\right|_{t=T}$$

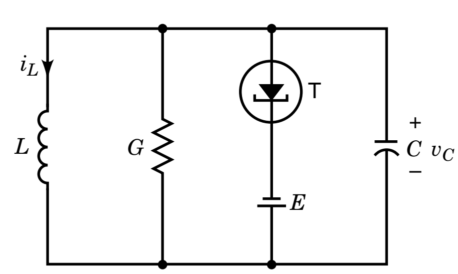

Figure 4. van der Pol oscillator.

Now, apply the Newton method to Eq. (15).

$$\begin{bmatrix} v_C^{j+1}(0) \\ T^{j+1} \end{bmatrix} = \begin{bmatrix} v_C^{j}(0) \\ T^{j} \end{bmatrix} - \left\{ \begin{bmatrix} 1 & 0 \\ 0 & 0 \end{bmatrix} - [\mathbf{J}^j] \right\}^{-1} \begin{bmatrix} v_C^j(0) - v_C^j(T^j) \\ i_L^j(0) - i_L(T^j) \end{bmatrix}$$

$$j = 0, 1, 2, \ldots$$

where

$$\mathbf{J}^j = \begin{bmatrix} \dfrac{\partial v_C(t)}{\partial v_C(0)} & \dfrac{\partial v_C(t)}{dt} \\ \dfrac{\partial i_L(t)}{\partial i_L(0)} & \dfrac{\partial i_L(t)}{\partial t} \end{bmatrix}\Bigg|_{t=T^j} \tag{16}$$

and using the relations

$$C\frac{dv_C}{dt} = i_C, \quad L\frac{di_L}{dt} = v_L$$

we have

$$\frac{\partial v_C(t)}{\partial t}\bigg|_{t=T^j} = \frac{1}{C} i_C\bigg|_{t=T^j}, \quad \frac{\partial i_L(t)}{\partial t}\bigg|_{t=T^j} = \frac{1}{L} v_L\bigg|_{t=T^j} \tag{17}$$

Thus, the first column of Eq. (16) is calculated by sensitivity analysis starting from the initial state $v_C(0) = 1$, and the second column is equal to the transient response at the jth iteration. The iteration will be continued until the variation becomes sufficiently small.

Note that in the case of oscillators, the convergence ratios of the time-domain method will usually be small compared with those for the forced circuits. The slow convergence seems to be due to the fact that although the period T is chosen as a variable in the shooting algorithm, it has a different property from the state variables.

Quasi-Periodic Solutions

Now, consider a system with two input signals.

$$\mathbf{f}(\dot{\mathbf{x}}, \mathbf{x}, \mathbf{y}, \omega_1 t, \omega_2 t) = \mathbf{0} \tag{18}$$

We assume that the ratio of ω_1 and ω_2 is an irrational number. Then, the steady-state solution will be a *quasi-periodic* function, which can be described by 2-fold Fourier expansion as follows:

$$\mathbf{x}(t) = \mathbf{g}_0(t) + \sum_{k=1}^{M} [\mathbf{g}_{2k-1}(t)\cos k\omega_2 t + \mathbf{g}_{2k}(t)\sin k\omega_2 t] \tag{19}$$

for a large M, where $\mathbf{g}_k(t)$, $k = 0, 1, 2, \ldots, 2M$ are period functions of $T_1 = 2\pi/\omega_1$. Let us choose $(2M + 1)$ data at $t = mT_1$, $m = 0, 1, 2, \ldots, 2M$ time points. Then, the steady-state solution satisfies the following relations:

$$\begin{aligned} \mathbf{x}(mT_1) = \mathbf{g}_0(0) &+ \sum_{k=1}^{M} (\mathbf{g}_{2k-1}(0)\cos mk\omega_2 T_1 \\ &+ \mathbf{g}_{2k}(0)\sin mk\omega_2 T_1) \quad m = 0, 1, 2, \ldots, 2M \end{aligned} \tag{20}$$

Thus, the coefficient $\mathbf{g}_k(0)$ can be solved as follows:

$$\mathbf{g}(0) = \Gamma^{-1}\mathbf{X}(T_1) \tag{21}$$

where

$$\Gamma = \begin{bmatrix} 1 & 1 & 0 & \cdots & 0 \\ 1 & \cos\omega_2 T_1 & \sin\omega_2 T_1 & \cdots & \sin M\omega_2 T_1 \\ 1 & \cos 2\omega_2 T_1 & \sin 2\omega_2 T_1 & \cdots & \sin 2M\omega_2 T_1 \\ \cdots & \cdots & \cdots & \cdots & \cdots \\ 1 & \cos 2M\omega_2 T_1 & \sin 2M\omega_2 T_1 & \cdots & \sin (2M)^2\omega_2 T_1 \end{bmatrix}$$

$$\mathbf{g}(0) = \begin{bmatrix} g_{1,0}(0) & g_{2,0}(0) & \cdots & g_{n,0}(0) \\ g_{1,1}(0) & g_{2,1}(0) & \cdots & g_{n,1}(0) \\ \cdots & \cdots & \cdots & \cdots \\ g_{1,2M}(0) & g_{2,2M}(0) & \cdots & g_{n,2M}(0) \end{bmatrix}$$

$$\mathbf{X}(T_1) = \begin{bmatrix} x_1(0) & x_2(0) & \cdots & x_n(0) \\ x_1(T_1) & x_2(T_1) & \cdots & x_n(T_1) \\ \cdots & \cdots & \cdots & \cdots \\ x_1(2MT_1) & x_2(2MT_1) & \cdots & x_n(2MT_1) \end{bmatrix}$$

If $\mathbf{x}(t)$ is the steady-state solution of Eq. (18), it must satisfy the following relation at $t = (2M + 1)T_1$:

$$\begin{aligned} \mathbf{x}((2M+1)T_1) &= \mathbf{g}_0(0) + \sum_{k=1}^{M} [\mathbf{g}_{2k-1}(0)\cos(2M+1)k\omega_2 T_1 \\ &\quad + \mathbf{g}_{2k}(0)\sin(2M+1)k\omega_2 T_1] \\ &= \mathbf{X}(T_1)^T[\boldsymbol{\Gamma}^{-1}]^T\boldsymbol{\Gamma}_{2M+1}^T \end{aligned} \tag{22}$$

$$\begin{aligned} \Gamma_{2M+1} = [&1\cos((2M+1)\omega_2 T_1)\sin((2M+1)\omega_2 T_1) \\ &\cdots\cos(M(2M+1)\omega_2 T_1)\sin(M(2M+1)\omega_2 T_1)] \end{aligned} \tag{23}$$

Thus, we have the *determining equation* for obtaining the quasi-periodic steady-state response:

$$\mathbf{F}(\mathbf{x}(0)) = \mathbf{x}((2M+1)T_1) - \mathbf{X}(T_1)^T[\boldsymbol{\Gamma}^{-1}]^T\boldsymbol{\Gamma}_{2M+1}^T = \mathbf{0} \tag{24}$$

Now, we apply the Newton method to Eq. (24).

$$\mathbf{x}^{j+1}(0) = \mathbf{x}^j(0) - \left[\frac{\partial \mathbf{F}(\mathbf{x}(0))}{\partial \mathbf{x}(0)}\right]^{-1}\Bigg|_{\mathbf{x}=\mathbf{x}^j(0)} \mathbf{F}(\mathbf{x}^j(0))$$

$$j = 0, 1, 2, \ldots \tag{25}$$

The Jacobian matrix is calculated by the *fundamental matrix solution* $\boldsymbol{\Phi}(t)$ of the sensitivity circuit as follows:

$$\begin{aligned} \frac{\partial \mathbf{F}(\mathbf{x}(0))}{\partial x(0)} &= \boldsymbol{\Phi}((2M+1)T_1) \\ &\quad - \sum_{k=0}^{2M} b_k \begin{bmatrix} \phi_{11}(kT_1) & \phi_{12}(kT_1) & \ldots & \phi_{1n}(kT_1) \\ \phi_{21}(kT_1) & \phi_{22}(kT_1) & \ldots & \phi_{2n}(kT_1) \\ \cdots & \cdots & \cdots & \cdots \\ \phi_{n1}(kT_1) & \phi_{n2}(kT_1) & \ldots & \phi_{nn}(kT_1) \end{bmatrix} \end{aligned} \tag{26}$$

where

$$[b_0 \quad b_1 \quad \cdots \quad b_{2M}]^T = [\boldsymbol{\Gamma}^{-1}]^T\boldsymbol{\Gamma}_{2M+1}^T$$

Note that, to implement one iteration, we need to calculate the transient response of Eq. (18) starting from $\mathbf{x}^j(0)$, and n times of the sensitivity analyses in the $[0, (2M + 1)T_1]$ period. The algorithm can be applied to the analysis of modulator amplitude and FM modulator circuits.

Example

Consider the differential-pair amplitude modulator circuit (26) shown in Fig. 5(a), where $e_1(t)$ and $e_2(t)$ denote the *carrier* and *signal* input, respectively. The steady-state waveform is shown in Fig. 5(b). The transistor is modeled by the Ebers-Moll model in the simulation.

Extrapolation Method

Although the time-domain method mentioned above can be applied to any kind of circuits, the efficiency will be decreased when the number of state variables is increased, because we need to solve the same number of sensitivity circuits as the state variables.

In this section, we show a *time-domain extrapolation method* (6) which only uses the transient response, without the need for any sensitivity analysis. Namely, we calculate $\mathbf{x}(T)$ by the numerical integration of Eq. (1) starting from $\mathbf{x}(0)$. Thus, we have

$$\mathbf{x}(T) = \mathbf{P}(\mathbf{x}(0)) \tag{27}$$

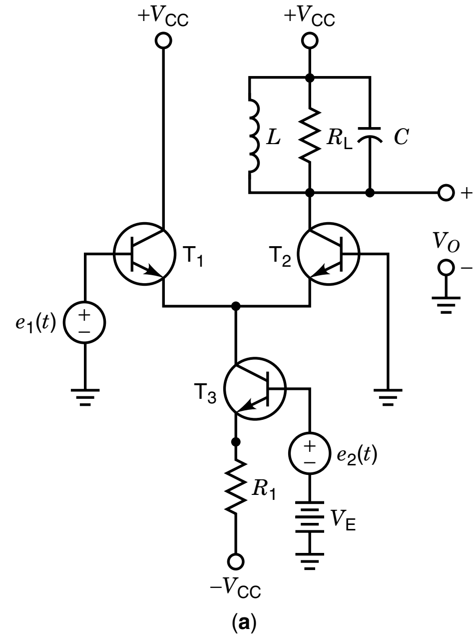

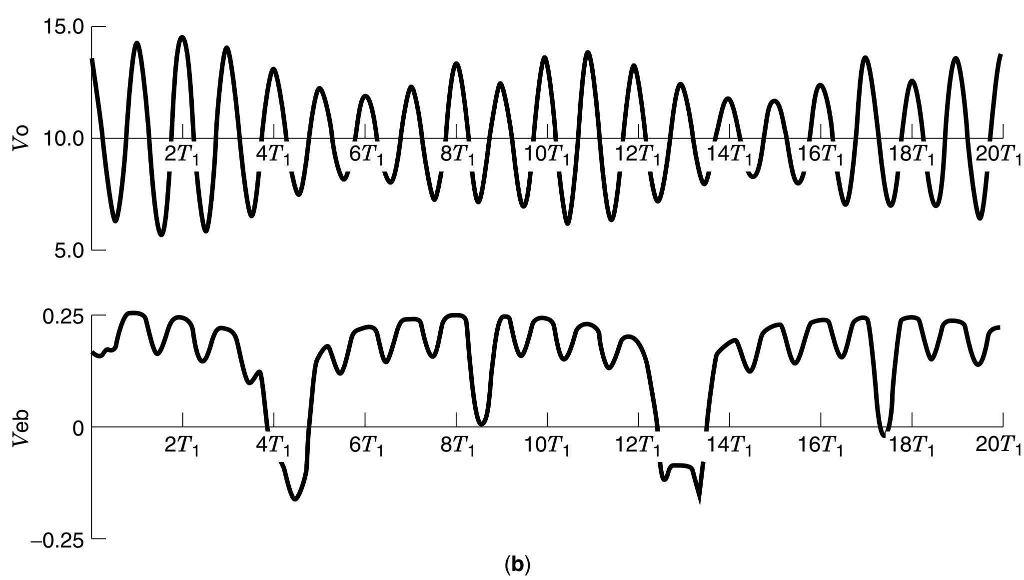

Figure 5. (a) Differential-pair amplitude modulator circuits; $V_{cc} = 10\,\text{V}$, $V_E = 5\,\text{V}$, $L = 2$ mH, $C = 500\,\text{pF}$, $R_L = 20\,\text{k}\Omega$; $e_1(t) = 0.01 \cos 10^6 t$ and $e_2(t) = 5.3 \cos 0.115 \times 10^6 t$, $i_d = 10^{-8}(e^{40v_d} - 1)$, $d = 99$. (b) Steady-state waveforms of v_0 and v_{eb} of T_1.

where $\mathbf{P}(\cdot)$ is called the *Poincaré map.* Now, set $\mathbf{x}^0(0) = \mathbf{x}(0)$, $\mathbf{x}^1(0) = \mathbf{x}(T)$, $\mathbf{x}^2(0) = \mathbf{x}(2T)$, ... Then, we have the following *contraction mapping:*

$$\mathbf{x}^{j+1}(0) = \mathbf{P}(\mathbf{x}^j(0)) \tag{28}$$

Observe that the contraction mapping is exactly the same as the *brute-force method.* There are some acceleration techniques based on the extrapolation method. The *ϵ-Algorithm* (6) is the simplest one as follows:

$$\begin{aligned} \epsilon_{-1}^{(j)} &= \mathbf{0}, \quad j = 0, 1, 2, \ldots \\ \epsilon_0^{(j)} &= \mathbf{x}^j(0), \quad j = 0, 1, 2, \ldots \\ \epsilon_k^{(n)} &= \epsilon_{k-1}^{(n-1)} + 1/(\epsilon_{k-1}^{(n)} - \epsilon_{k-1}^{(n-1)}) \\ & k = 1, 2, \ldots, \quad n = k, k+1, \ldots \end{aligned} \tag{29}$$

Thus, the kth-order solution is given by

$$\mathbf{x}^k(0) = \epsilon_{2k}^{(n)}, \quad n \geq 2k \tag{30}$$

where we need to estimate the inverse of the vectors. The Samelson inverse (27) is defined for a vector $\boldsymbol{v}$

$$\boldsymbol{v}^{-1} = \boldsymbol{v}/\boldsymbol{v}^T\boldsymbol{v} \tag{31}$$

The extrapolation method is very easy to implement, and it is efficient for the steady-state analysis of nonlinear circuits with *few* reactive elements giving rise to slow decaying transients.

FREQUENCY-DOMAIN APPROACH

The steady-state waveform of a nonlinear circuit can always be described by a trigonometric polynomial. Each harmonic component must respectively balance in the circuit equation. Thus, if we consider the M frequency components plus the dc component, we have a set of $N(2M + 1)$ algebraic equations for N nonlinear elements. The equations can solved by the Newton and/or the relaxation methods. Note that FFT (the fast Fourier transformation) is often used for the Fourier transformation in the frequency-domain approaches.

Harmonic Balance Method

The *harmonic balance method* is widely used in the *frequency-domain approach* of the steady-state analysis of nonlinear circuits. The ideas are based on the *Galerkin's procedure* which states that the periodic steady-state solution can be approximated by a finite number of trigonometric polynomial (9,17). Now, consider a nonlinear periodic system

$$\frac{d\mathbf{x}}{dt} = \mathbf{f}(\mathbf{x}, \omega t) \tag{32}$$

To determine the periodic solution of Eq. (32), we first take a trigonometric polynomial

$$\mathbf{x}_M(t) = \mathbf{X}_0 + \sum_{k=0}^{M}(\mathbf{X}_{2k-1}\cos k\omega t + \mathbf{X}_{2k}\sin k\omega t) \tag{33}$$

with undetermined coefficients ($\mathbf{X}_0$, $\mathbf{X}_1$, . . . , $\mathbf{X}_{2M-1}$, $\mathbf{X}_{2M}$). Substituting Eq. (33) into Eq. (32), we consider the following equation with the undetermined coefficients.

$$\begin{aligned} \frac{d\mathbf{x}_M}{dt} &= \frac{1}{T}\int_0^T \mathbf{f}(\mathbf{x}_M(\tau), \tau)\,d\tau \\ &+ \frac{1}{2T}\sum_{k=1}^{M}\left(\cos k\omega t \cdot \int_0^T \mathbf{f}(\mathbf{x})M(\tau), \tau)\cos k\omega\tau\,d\tau \right. \\ &\left. + \sin k\omega t \cdot \int_0^T \mathbf{f}(\mathbf{x}_M(\tau), \tau)\sin k\omega\tau\,d\tau\right) \end{aligned} \tag{34}$$

From Eq. (34), we have

$$\mathbf{F}_0(\alpha) = \frac{1}{T}\int_0^T \mathbf{f}(\mathbf{x}_M(\tau), \tau)\,d\tau = \mathbf{0} \tag{35a}$$

$$\mathbf{F}_{2k-1}(\alpha) = \frac{1}{2T}\int_0^T \mathbf{f}(\mathbf{x}_M(\tau), \tau)\cos k\omega\tau\,d\tau - k\mathbf{X}_{2k} = \mathbf{0} \tag{35b}$$

$$\mathbf{F}_{2k}(\alpha) = \frac{1}{2T}\int_0^T \mathbf{f}(\mathbf{x}_M(\tau), \tau)\sin k\omega\tau\,d\tau + k\mathbf{X}_{2k-1} = \mathbf{0} \tag{35c}$$

$$k = 1, 2, \ldots, M$$

where $\alpha = (\mathbf{X}_0, \mathbf{X}_1, \ldots, \mathbf{X}_{2M-1}, \mathbf{X}_{2M})$. Suppose Eq. (35) has a solution $\overline{\alpha} = (\overline{\mathbf{X}}_0, \overline{\mathbf{X}}_1, \ldots, \overline{\mathbf{X}}_{2M-1}, \overline{\mathbf{X}}_{2M})$. Then, the approximate solution is given by

$$\overline{\mathbf{x}}_M(t) = \overline{\mathbf{X}}_0 + \sum_{k=0}^{M}(\overline{\mathbf{X}}_{2k-1}\cos k\omega t + \overline{\mathbf{X}}_{2k}\sin k\omega t) \tag{36}$$

which is called the *Galerkin approximation* of order M, and Eq. (35) is the determining equation of the Mth order Galerkin approximation. The existence of an exact isolated periodic solution and the error bound is shown in Ref. 9.

Example

To understand the ideas of the *harmonic balance method* (10), consider a simple LRC circuit with a nonlinear resistor as shown in Fig. 6. Assume the characteristic of the nonlinear resistor is given by

$$i_G = \hat{\imath}_G(v) \tag{37}$$

and the input voltage sources given by

$$e(t) = E_m\cos(\omega t + \theta) \tag{38}$$

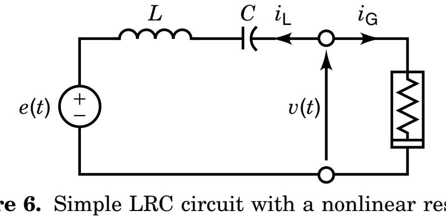

Figure 6. Simple LRC circuit with a nonlinear resistor.

Suppose the voltage at the nonlinear resistor is a trigonometric polynomial as follows:

$$v(t) = V_0 + \sum_{k=1}^{M} (V_{2k-1} \cos k\omega t + V_{2k} \sin k\omega t) \tag{39}$$

Then, the response of the linear subcircuit in the left-hand side is easily calculated by the phasor technique

$$i_L(t) = \sum_{k=1}^{M} (I_{L,2k-1} \cos k\omega t + I_{L,2k} \sin k\omega t) \tag{40}$$

where

$$I_{L,1} = \frac{\omega C(V_2 + E_m \sin\theta)}{1-\omega^2 LC}, \quad I_{L,2} = \frac{\omega C(-V_1 + E_m \cos\theta)}{1-\omega^2 LC}$$
$$I_{L,2k-1} = \frac{k\omega C V_{2k}}{1-(k\omega)^2 LC}, \quad I_{L,2k} = -\frac{k\omega C V_{2k-1}}{1-(k\omega)^2 LC}$$
$$k = 2, 3, \ldots, M$$

On the other hand, the response of nonlinear resistor to $v(t)$ is described by a trigonometric polynomial as follows:

$$i_G(t) = I_{G,0} + \sum_{k=1}^{M} (I_{G,2k-1} \cos k\omega t + I_{G,2k} \sin k\omega t) \tag{41}$$

The steady-state waveform needs to satisfy the following condition:

$$i_L(t) + i_G(t) = 0 \tag{42}$$

Thus, we have the following determining equations for each frequency component:

$$I_{G,0}(V_0, V_2, \ldots, V_{2M}) = 0 \tag{42a}$$
$$I_{L,2k-1}(V_{2k-1}, V_{2k}) + I_{G,2k-1}(V_0, V_2, \ldots, V_{2M}) = 0 \tag{42b}$$
$$I_{L,2k}(V_{2k-1}, V_{2k}) + I_{G,2k}(V_0, V_2, \ldots, V_{2M}) = 0 \tag{42c}$$
$$k = 1, 2, \ldots, M$$

It can be solved by the Newton Raphson method:

$$\mathbf{V}^{j+1} = \mathbf{V}^j - [\mathbf{J}_L + \mathbf{J}_G(\mathbf{V}^j)]^{-1}[\mathbf{I}_L(\mathbf{V}^j) + \mathbf{I}_G(\mathbf{F}^j)], \quad j = 1, 2, 3, \ldots \tag{43}$$

where $\mathbf{V} = [V_0, V_1, \ldots, V_{2M}]^T$, $\mathbf{I}_L(\mathbf{V}) = [I_{L,0}, I_{L,1}, \ldots, I_{L,2M}]^T$, $\mathbf{I}_G(\mathbf{V}) = [I_{G,0}, I_{G,1}, \ldots, I_{G,2M}]^T$, and $\mathbf{J}_L = \mathrm{diag}[0, \mathbf{Y}_1(\omega), \mathbf{Y}_2(2\omega), \ldots, \mathbf{Y}_M(M\omega)]$ where

$$\mathbf{Y}_k(k\omega) = \begin{bmatrix} 0 & y_I(k\omega) \\ -y_I(k\omega) & 0 \end{bmatrix}, \quad \text{for } y_I(k\omega) = \frac{k\omega C}{1-(k\omega)^2 LC}$$

On the other hand, the Jacobian matrix of the nonlinear resistor is given by

$$\mathbf{J}_G \equiv \begin{bmatrix} J_{G,0,0} & J_{G,0,1} & \cdots & J_{G,0,2M} \\ J_{G,1,0} & J_{G,1,1} & \cdots & J_{G,1,2M} \\ \cdots & \cdots & \cdots & \cdots \\ J_{G,2M,0} & J_{G,2M,1} & \cdots & J_{G,2M,2M} \end{bmatrix} \tag{44}$$

where

$$\begin{aligned} J_{G,0,0} &= \frac{1}{T}\int_0^T \frac{\partial \hat{\imath}_G}{\partial v}\,dt \\ J_{G,2m-1,2k-1} &= \frac{1}{2T}\int_0^T \frac{\partial \hat{\imath}_G}{\partial v} \cos m\omega t \cdot \cos k\omega t\,dt \\ J_{G,2m-1,2k} &= \frac{1}{2T}\int_0^T \frac{\partial \hat{\imath}_G}{\partial v} \cos m\omega t \cdot \sin k\omega t\,dt \\ J_{G,2m,2k-1} &= \frac{1}{2T}\int_0^T \frac{\partial \hat{\imath}_G}{\partial v} \sin m\omega t \cdot \cos k\omega t\,dt \\ J_{G,2m,2k} &= \frac{1}{2T}\int_0^T \frac{\partial \hat{\imath}_G}{\partial v} \sin m\omega t \cdot \sin k\omega t\,dt \\ k &= 1, 2, \ldots, M, \quad m = 1, 2, \ldots, M \end{aligned} \tag{45}$$

Therefore, we must apply a total of $(2M + 1)$ times Fourier expansions for getting the Jacobian matrix.

Note that the scale of the determining equations is $N(2M + 1)$ for a circuit with N nonlinear elements. Hence, the efficiency of the frequency-domain approach is rapidly decreased as the number of nonlinear elements increases and their nonlinearities become strong.

Frequency-Domain Relaxation Method

To focus on the main idea of the frequency-domain relaxation method, consider the circuit shown in Fig. 7(a), where N_L denotes a linear subnetwork and G denotes a voltage-controlled nonlinear resistor described by

$$i_G = \hat{\imath}_G(v) \tag{46}$$

Assuming the inputs have multiple frequencies $\omega_1, \omega_2, \ldots, \omega_r$, then the voltage across the nonlinear resistor can generally be assumed to have the form

$$v(t) = V_0 + \sum_{k=1}^{M} (V_{2k-1} \cos \nu_k t + V_{2k} \sin \nu_k t) \tag{47}$$

where

$$\nu_k = m_{1k}\omega_1 + m_{2k}\omega_2 + \cdots + m_{rk}\omega_r \tag{48}$$

and the integers satisfy $|m_{1k}| < B_1$, $|m_{2k}| < B_2, \ldots, |m_{rk}| < B_k$ for some sufficiently large B. Assuming that the original circuit in Fig. 7(a) has a unique steady-state solution described by Eq. (47), then $v(t)$ satisfies

$$F(v(t)) \equiv i_L(t) + i_G(t) = 0 \tag{49}$$

where $i_L(t)$ and $i_G(t)$ denote the currents in the linear and nonlinear subnetworks in Fig. 7(b).

Let us calculate the steady-state solution using an iterational technique in the frequency-domain. Assume the solution at the jth iteration is given by

$$v^j(t) = V_0^j + \sum_{k=1}^{M} (V_{2k-1}^j \cos \nu_k t + V_{2k}^j \sin \nu_k t) \tag{50}$$

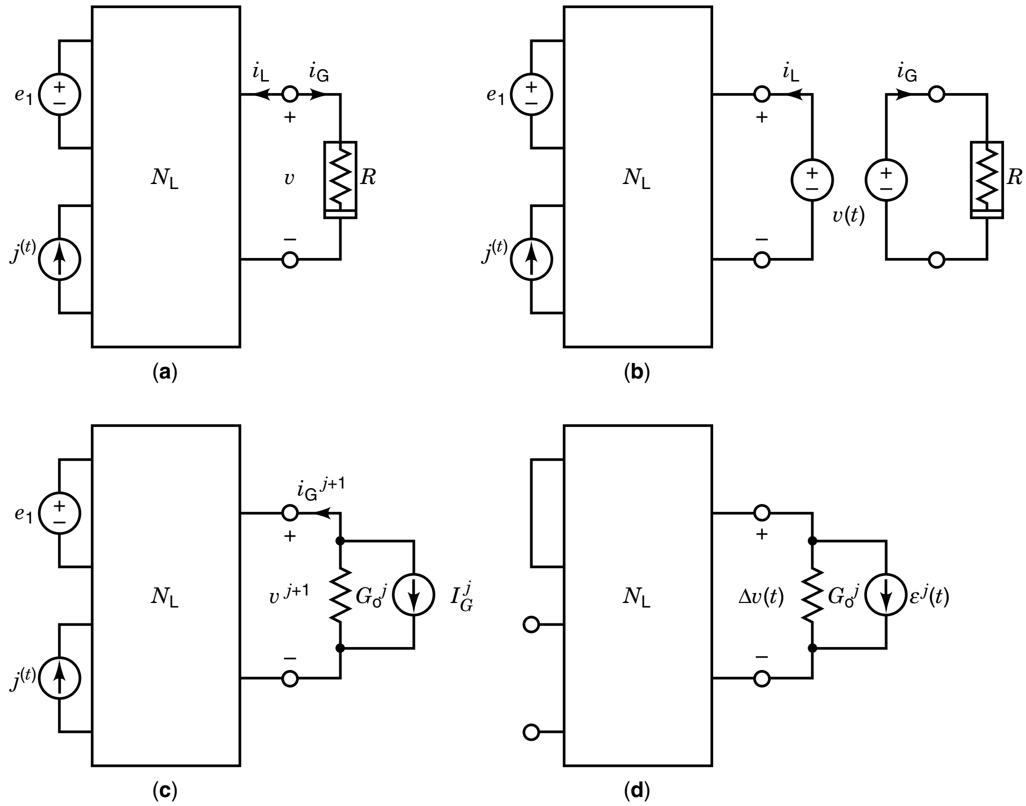

Figure 7. Relaxation circuit: (a) Nonlinear circuit with a voltage-controlled resistor; (b) Partioning into a linear and a nonlinear subcircuit; (c) Approximation of the linear time-invariant equivalent circuit, where $j^j(t) = \hat{\imath}_G(v^j) - G_0 v^j$; (d) Sensitivity circuit.

To evaluate the solution at the $(j + 1)$th iteration, let

$$v^{j+1}(t) = v^j(t) + \Delta v(t) \tag{51}$$

where

$$\Delta v(t) = \Delta V_0 + \sum_{k=1}^{M} (\Delta V_{2k-1} \cos \nu_k t + \Delta V_{2k} \sin \nu_k t) \tag{52}$$

is some appropriate perturbation to be determined below. Substituting v^{j+1} from Eq. (51) into Eq. (49), and neglecting the higher-order terms of Δv in the Taylor expansion of $\hat{\imath}_G(t)$, we obtain for the weakly nonlinear system

$$\begin{aligned} F(v^j + \Delta v) &= \mathscr{L}(v^j + \Delta v) + \mathscr{S}(e(t),\ j(t)) + \hat{\imath}_G(v^j + \Delta v) \\ &\approx \mathscr{L}(v^j + \Delta v) + \mathscr{S}(e(t),\ j(t)) + \hat{\imath}_G(v^j) + G^j(t)\,\Delta v \qquad \text{(53a)} \\ &\approx \mathscr{L}(v^j + \Delta v) + \mathscr{S}(e(t),\ j(t)) + \hat{\imath}_G(v^j) + G_0^j\,\Delta v \qquad \text{(53b)} \end{aligned}$$

where

$$G^j(t) \equiv \left.\frac{\partial \hat{\imath}_G}{\partial v}\right|_{v=v^j} = G_0^j + \sum_{k=1}^{M} (G_{2k-1}^j \cos \nu_k t + G_{2k}^j \sin \nu_k t) \tag{54}$$

The symbols $\mathscr{L}$ and $\mathscr{S}$ denote linear operators which transform the voltage $v(t)$ and the sources $(e(t), j(t))$ respectively into the time-domain responses of the linear subnetwork in Fig. 7(b). Observe that since Eq. (53a) is a time-varying system, it is not easy to solve. Thus, we rewrite it as Eq. (53b), where only G_0^j is used instead of $G^j(t)$. It can be further written in the following form:

$$\mathscr{L}(\Delta v) + G_0^j \Delta v = -\mathscr{L}(v^j) - \mathscr{S}(e(t),\ j(t)) - \hat{\imath}_G(v^j) \tag{55}$$

Observe that the convergence ratio will depend on the nonlinearity given by the difference $G^j(t) - G_0^j$. Now, we define the *residual error current*

$$\epsilon^j(t) \equiv \mathscr{L}(v^j) + \mathscr{S}(e(t),\ j(t)) + \hat{\imath}_G(v^j) \tag{56}$$

Thus, we can obtain the equivalent circuits of Fig. 7(c) and (d) from the relations Eq. (53b) and Eq. (55), respectively, where

$$j^j(t) = \hat{\imath}_G(v^j) - G_0^j v^j$$

We call the circuits *relaxation circuits,* which can be easily solved by the phasor technique for each frequency component. The iteration will be continued until the variation satisfies

$$\sum_{k=0}^{2M} |V_k^j - V_k^{j+1}| < \epsilon \tag{57}$$

for some prescribed small tolerance ϵ.

Remark: the frequency-domain relaxation method presented above can be efficiently applied to weakly nonlinear

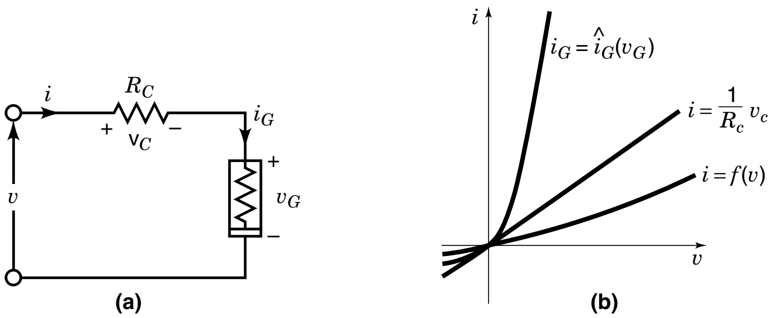

Figure 8. Compensation technique: (a) Series compensation by R_c; (b) a schematic diagram of weakening the nonlinearity.

circuits. However, many semiconductor devices such as diodes and transistors are characterized by strong nonlinearities, so that the convergence of our relaxation method may not be guaranteed. In such cases, we recommend introducing compensation resistors R_c in series for the nonlinear subnetwork and $-R_c$ for the linear subnetwork, which plays a very important role in weakening the nonlinearity, as shown in Fig. 8.

Hybrid Harmonic Balance Method

In the above section, we discussed a *frequency-domain relaxation method,* where each nonlinear element is replaced by the time-invariant linear element with the associate source at each iteration. Thus, every frequency component can be calculated by the phasor technique. We propose here an efficient *hybrid relaxation method* based on both the time-domain and the frequency-domain approaches (20,23). At the first step, a given circuit is partitioned into subnetworks using substitution sources (28), where one group N_1 contains only *linear* or weakly elements and the other N_2 *nonlinear* elements, as shown in Fig. 9. From the computational efficiency, we recommend to partition the circuit such that N_1 contains as many capacitors and inductors as possible, and N_2 as many resistive elements as possible. Thus, the steady-state responses of N_1 are calculated by the frequency-domain method, and those of N_2 by a time-domain approach. If those two responses at the partitioning points have the same waveforms, then the substitution sources give rise to a steady-state response. To understand the basic ideas behind the *hybrid harmonic balance method,* consider the simple circuit shown in Fig. 9(a). Now, approximate the substitution voltage sources in Fig. 9(b) as follows:

$$\mathbf{v}(t) = \mathbf{V}_0 + \sum_{k=0}^{M} (\mathbf{V}_{2k-1} \cos \nu_k t + \mathbf{V}_{2k} \sin \nu + kt) \tag{58}$$

where $\mathbf{v} = [v_1,\ v_2]^T$, $\mathbf{V} = [V_1, V_2]^T$ and ν_k is equal to a linear combination of the input frequencies $\omega_1, \omega_2, \ldots, \omega_r$, namely

$$\nu_k \equiv m_{1k}\omega_1 + m_{2k}\omega_2 + \cdots + m_{rk}\omega_r \tag{59}$$

where $m_{1k}, m_{2k}, \ldots, m_{rk}$ are integers satisfying

$$|m_{ik}| \le B_k, \quad i = 1, \ldots, r; \quad k = 1, \ldots, M \tag{60}$$

Remark: if the relations among $\omega_1, \omega_2, \ldots, \omega_r$ are *irrational,* $\mathbf{v}(t)$ in Eq. (58) will be a quasi-periodic function, and it is not easy to solve the circuit. In this case, consider calculating an approximate periodic solution, and put

$$\omega_1 \approx n_1 \Delta\omega, \omega_2 \approx n_2 \Delta\omega, \ldots, \omega_r \approx n_r \Delta\omega \tag{61}$$

Then, the period is given by

$$T = \frac{2\pi}{n\Delta\omega}; \quad n = \mathrm{GCM}\{n_1, n_2, \ldots, r\} \tag{62}$$

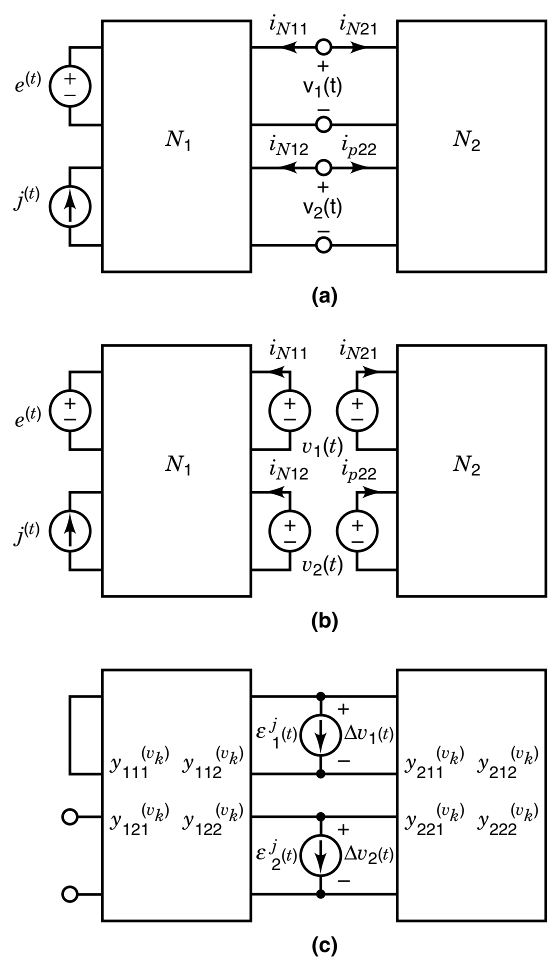

Figure 9. Circuit partitioning: (a) A given circuit; (b) Partition into two groups of N_1 and N_2; (c) The sensitivity circuit for calculating the variation Δv_1, Δv_2.

and the steady-state solution will satisfy the following *determining equation:*

$$\mathbf{F}(\mathbf{v}) = \mathbf{i}_{N1}(\mathbf{v}, \mathbf{e}(t), \mathbf{j}(t)) + \mathbf{i}_{N2}(\mathbf{v}) = \mathbf{0} \tag{63}$$

where $\mathbf{F} = [F_1, F_2]^T$, $\mathbf{i} = [i_1, i_2]^T$. Let us solve the steady-state solution satisfying Eq. (63) by an iteration method, and assume the waveform at the jth iteration is expressed by

$$\mathbf{v}^j(t) = \mathbf{V}_0^j + \sum_{k=0}^{M} (\mathbf{V}_{2k-1}^j \cos \nu_k t + \mathbf{V}_{2k}^j \sin \nu_k t) \tag{64}$$

We first solve the subnetworks N_1 with the *frequency-domain relaxation method.* Of course, we can solve them by the *phasor technique* if they are linear. The subnetworks N_2 are solved by some time-domain method. If the damping coefficient is sufficiently large, we can solve it by the *brute-force method.* Otherwise, we need to choose the Newton method (2) or the extrapolation method (6). To calculate the solution at the $(j+1)$th iteration, assume the solution

$$\mathbf{v}^{j+1}(t) = \mathbf{v}^j(t) + \Delta\mathbf{v}(t) \tag{65}$$

where $\Delta\mathbf{v}(t)$ is a variational voltage waveform described by

$$\Delta\mathbf{v}(t) = \Delta\mathbf{V}_0 + \sum_{k=0}^{M} (\Delta\mathbf{V}_{2k-1} \cos \nu_k t + \Delta\mathbf{V}_{2k} \sin \nu_k t) \tag{66}$$

Substituting $\mathbf{v}^{j+1}(t)$ from Eq. (65) into Eq. (63), we obtain

$$\begin{aligned}\mathbf{F}(\mathbf{v}^j + \Delta\mathbf{v}) &= \mathbf{i}_{N1}(\mathbf{v}^{j+1}, \mathbf{e}(t), \mathbf{j}(t)) + \mathbf{i}_{N2}(\mathbf{v}^{j+1}) \\ &\approx \mathbf{Y}_{N1,0}^j(\Delta\mathbf{v}) + \mathbf{Y}_{N2,0}^j(\Delta\mathbf{v}) + \epsilon^j(t) = \mathbf{0}\end{aligned} \tag{67}$$

where the *residual error* $\epsilon^j(t)$ is defined by

$$\begin{aligned}\epsilon^j(t) &\equiv \mathbf{i}_{N1}(\boldsymbol{v}^j, \boldsymbol{e}(t), \boldsymbol{j}(t)) + \mathbf{i}_{N2}(\mathbf{v}^j) \\ &= \epsilon_0^j + \sum_{k=0}^{M} (\epsilon_{2k-1}^j \cos \nu_k t + \sin \nu_k t)\end{aligned} \tag{68}$$

$\mathbf{Y}_{N1,0}^j(\Delta\mathbf{v})$ and $\mathbf{Y}_{N2,0}^j(\Delta\mathbf{v})$ are the time-invariant linear operators obtained from the sensitivity circuit at the jth iteration. Since in many practical applications, the differences of the linear operators in each iteration are small enough, we can approximate them with those at the zeroth iteration, which correspond to the incremental admittance matrices at the operating point. Thus, the variational values are calculated by

$$[\overline{\mathbf{Y}}_{N1,0}(j\nu_k) + \overline{\mathbf{Y}}_{N2,0}(j\nu_k)](\Delta\mathbf{V}_{2k-1} + j\Delta\mathbf{V}_{2k}) = \epsilon_{2k-1}^j + j\epsilon_{2k}^j \qquad k = 1, 2, \ldots, M \tag{69}$$

where $\overline{\mathbf{Y}}$ is the complex conjugate. The iteration is continued until the variation satisfies

$$\|\Delta\mathbf{V}\| < \delta \tag{70}$$

for a given small δ.

In order to determine the accuracy of the solution, we also need to evaluate the *residual error* given by

$$\begin{aligned}\epsilon^j &= \sqrt{\frac{1}{T}\int_0^T (\mathbf{i}_{N1}(\mathbf{v}^j, \mathbf{e}(t), \boldsymbol{j}(t)) + \mathbf{i}_{N2}(\mathbf{v}^j))^2\, dt} \\ &= \sqrt{\sum_{k=2M+1}^{\infty} |\mathbf{I}_{N1,k}^2 + \mathbf{I}_{N2,k}^2|^2}\end{aligned} \tag{71}$$

The hybrid harmonic balance method needs to apply the frequency-domain relaxation method to the weakly nonlinear subnetworks N_1, and the time-domain method to the nonlinear subnetworks N_2 at each iteration. The variation $\Delta\mathbf{v}(t)$ can be simply obtained by the use of the admittance matrices. Therefore, the algorithm is very efficient compared with other algorithms. The practical circuits are composed of many kinds of subnetworks such as amplifiers, filters, multipliers and pulse circuits, and so on. For example, consider a modulator circuit composed of a multiplier, filter, and amplifier, where the multiplier is only a nonlinear subnetwork, and the filter and amplifier are the linear subnetworks for small signals even if it contains nonlinear elements such as transistors. The response of the linear subnetwork can be easily calculated by the phasor technique such as the SPICE ac-analysis tool. Furthermore, it is sometimes possible to partition the circuits into linear and nonlinear subnetworks such that the nonlinear subnetworks have large damping terms. In these cases, we only need the time-domain analyses of the nonlinear subnetworks at each iteration. Thus, the algorithm (20) will become much more simple and efficient.

Example

Consider a mixer circuit shown in Fig. 10. Let us partition the circuit at (a, a') and (b, b'). Then, the linear subnetworks are only capacitors C_1 and C_2, and the rest is assumed to be the nonlinear subnetwork. We used two periods of the brute-force method for the time-domain analysis of the nonlinear subnetwork. The convergence ratio is shown in Fig. 10(c), and the frequency spectrum Fig. 10(b). Note that we obtained the same result in 100 periods with the transient analysis of SPICE. On the other hand, our hybrid method could calculate the steady-state response in a total of 12 periods with the time-domain brute-force method to the nonlinear subnetwork.

SMALL SIGNAL ANALYSIS METHOD FOR PERIODIC NONLINEAR CIRCUITS

Among nonlinear circuits with multiple frequency excitations, there is a significant class of circuits with two excitations where one of the excitations is large and the other is small. Frequency converters normally have two excitations; one is a strong local oscillator (LO) signal, the other is a radio frequency (RF) signal. Modulators and switched capacitor filters (SCFs) also belong to this class. Figure 11 shows a circuit model of these circuits. Small signal responses for these circuits are one of the prime points of interest for circuit design. This section describes numerically small signal analysis methods for periodically operating nonlinear circuits with a periodic large excitation.

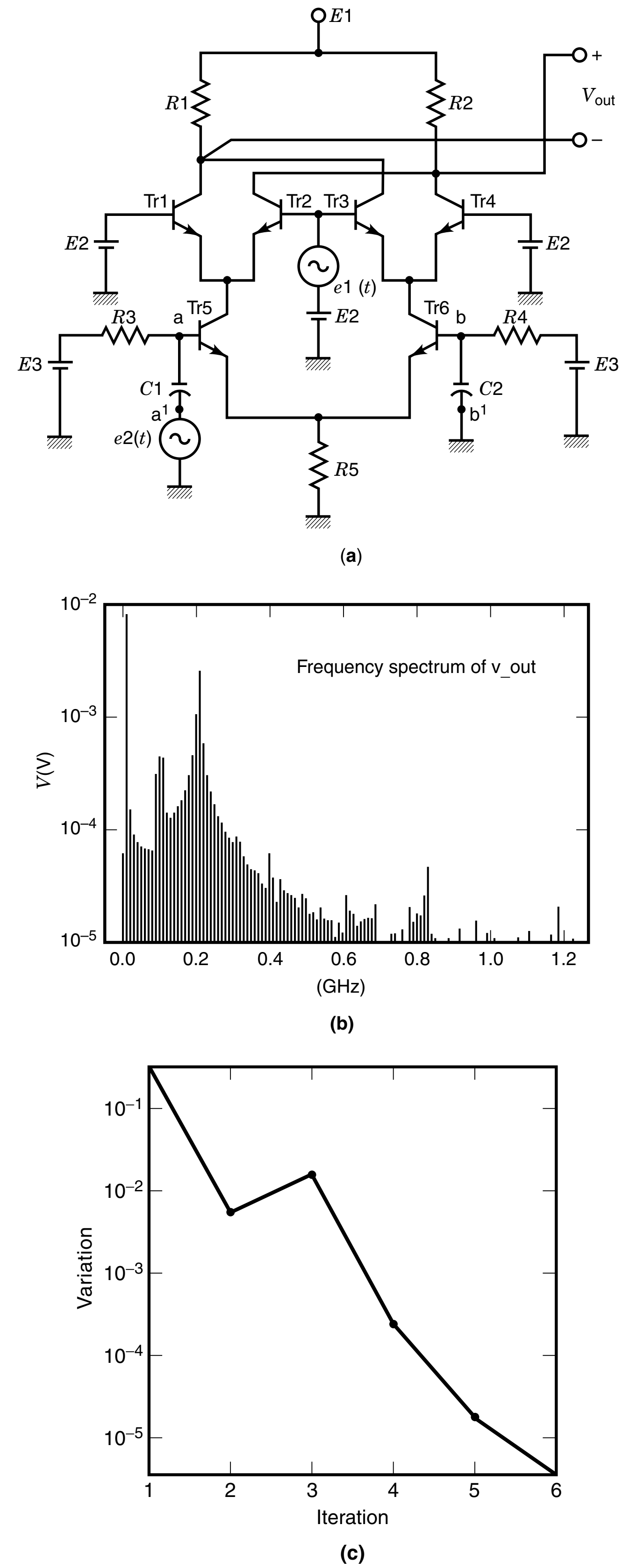

Figure 10. (a) A mixer circuit $R_1 = R_2 = 100\ \Omega$, $R_3 = R_4 = 10\ \text{k}\Omega$, $C_1 = C_2 = 10$ nF, $E_1 = 5$ V, $E_2 = 2.5$ V, $E_3 = 12$ V $e_1(t) = 0.03 \sin 2\pi \times 0.11 \times 10^9 t$, $e_2(t) = 0.02 \sin 2\pi \times 0.1 \times 10^9 t$. (b) Frequency spectrum of output waveform; (c) Convergence ratio.

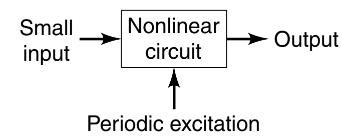

Figure 11. A circuit model.

Linear Periodic Time-Varying Circuit

Small signal analyses for periodic nonlinear circuits can be expected to be efficient if the circuits are modeled as the corresponding *linear periodic time-varying* (LPTV) circuits for small signals as shown in Fig. 12. The LPTV circuit can be obtained by applying the perturbation technique to the periodic steady-state solution of the nonlinear circuit without an input signal (29).

Consider a nonlinear system with a periodic large excitation:

$$\mathbf{f}(\mathbf{x}(t),\ \dot{\mathbf{x}}(t)) = \mathbf{e}(t) \tag{72}$$

where $\dot{\mathbf{x}}(t)$ denotes the time derivative of $\mathbf{x}(t)$, and $\mathbf{e}(t)$ is a large excitation of period T. The periodic large excitation might be a clock signal for SCFs or an LO signal for mixer circuits, for example.

It is assumed that the system represented by Eq. (72) has a stable periodic solution $\mathbf{x}_{st}(t)$ with period T for all t;

$$\mathbf{x}_{st}(t - T) = \mathbf{x}_{st}(t)$$

The steady-state periodic solution is computed using the shooting method (2,5), harmonic balance method (10,11), or simply using transient analysis.

Applying the perturbation technique to the periodic solution of the nonlinear system of Eq. (72), we have

$$\mathbf{g}(t)\,\Delta\mathbf{x}(t) + \mathbf{c}(t)\,\Delta\dot{\mathbf{x}}(t) = \mathbf{u}(t) \tag{73}$$

where

$$\mathbf{u}(t) = \delta\mathbf{e}(t)$$
$$\mathbf{g}(t) = \left.\frac{\partial\mathbf{f}(t)}{\partial\mathbf{x}(t)}\right|_{\mathbf{x}(t)=\mathbf{x}_{st}(t)}$$
$$\mathbf{c}(t) = \left.\frac{\partial\mathbf{f}(t)}{\partial\dot{\mathbf{x}}(t)}\right|_{\dot{\mathbf{x}}(t)=\dot{\mathbf{x}}_{st}(t)}$$

Equation (73) is an LPTV circuit as $\mathbf{g}(t)$ and $\mathbf{c}(t)$ are T-periodic.

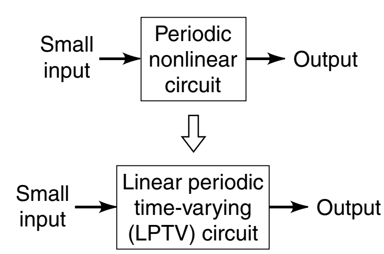

Figure 12. Modeling of a periodic nonlinear circuit by an LPTV circuit.

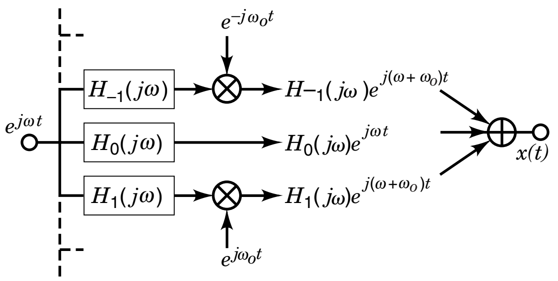

Figure 13. Representation of a periodic time-varying transfer function by LTI filters and mixers.

Transfer Function of LPTV Circuit

The small signal response $\Delta\mathbf{x}(t)$ for Eq. (73) can be written using the LPTV transfer function (30).

$$\Delta\mathbf{x}(t) = \frac{1}{2\pi}\int_{-\infty}^{\infty}\mathbf{H}(j\Omega,\ t)\mathbf{U}(j\Omega)e^{j\Omega t}\,d\Omega$$

where $\mathbf{H}(j\Omega,\ t)$ is the LPTV transfer function and $\mathbf{U}(j\Omega)$ is the Fourier transform of the input signal. The transfer function is represented by a matrix whose dimension is the number of variables. For simplicity, we use one variable after this.

Assuming that a unit input signal is $u(t) = e^{j\omega t}$, a steady-state response $\Delta x(t)$ to $u(t)$ becomes

$$\Delta x(t) = H(\omega,\ t)e^{j\omega t}$$

Expanding $H(\omega,\ t)$ into a Fourier series using the periodicity, we have

$$\Delta x(t) = \sum_{l=-\infty}^{\infty} H_l(\omega)e^{j(\omega+l\omega_0)t}$$

where $\omega_o = 2\pi/T$. The Fourier coefficients $H_l(\omega)$ represent *linear time-invariant* (LTI) filters. Figure 13 shows a representation of an LPTV transfer function by LTI filters and mixers. It can be considered that the first Fourier coefficient $H_0(\omega)$ represents a transfer function without frequency translation, while $H_l(\omega)$ for $l \neq 0$ represents transfer functions with frequency translation from ω to $\omega + l\omega_o$.

For example, $H_0(\omega)$ is used for the calculation of the baseband frequency characteristics of an SCF. $H_1(\omega)$ is used for the calculation of conversion gain of an up-conversion mixer circuit and $H_{-1}(\omega)$ is used for down-conversion mixer circuits.

The Fourier coefficients $H_l(\omega)$ of an LPTV transfer function can be calculated by solving LPTV differential Eq. (73). There are two major techniques. One is the frequency-domain method using conversion matrices (31–33) based on the harmonic balance technique. The other is the time-domain method (16,34) using numerical integration. The time-domain method is described briefly here.

In the time-domain method, an LPTV transfer functions at discrete times, that is, $H(j\omega,\ \tau_m)$, $m = 1, 2, \ldots, P$, is calculated by using periodic time-varying parameters, where the variable definitions are as follows:

$$T = \sum_{m=1}^{P} h_m, \quad \tau_m = \sum_{k=1}^{m} h_k, \quad \tau_p = T, \quad \tau_0 = 0$$

The periodic time-varying parameters are obtained during numerical integration for one period of the periodic nonlinear circuits. Fourier coefficients $H_l(\omega)$ are calculated from LPTV transfer functions at discrete times over one period.

Next, consider the calculation of LPTV transfer functions at discrete times. Applying a unit complex sinusoidal signal and evaluating Eq. (73) at $t = nT + \tau_m$, we have

$$\mathbf{g}_m\,\Delta\mathbf{x}(nT+\tau_m) + \mathbf{c}_m\Delta\dot{\mathbf{x}}(nT+\tau_m) = \mathbf{u}e^{j\Omega(nT+\tau_m)} \tag{74}$$

where $\mathbf{g}_m = \mathbf{g}(nT + \tau_m)$, $\mathbf{c}_m = \mathbf{c}(nT + \tau_m)$ and $\mathbf{u}$ is a vector which indicates where the input signal is connected.

The differential Eq. (74) is numerically solved by applying the backward Euler method to give

$$\left(\mathbf{g}_m + \frac{\mathbf{c}_m}{h_m}\right)\Delta\mathbf{x}(nT+\tau_m) - \frac{\mathbf{c}_m}{h_m}\Delta\mathbf{x}(nT+\tau_{m-1}) = \mathbf{u}e^{j\Omega(nT+\tau_m)} \tag{75}$$

The relationship between $\mathbf{H}(\Omega,\ \tau_m)$ and $\Delta\mathbf{x}(nT + \tau_m)$ can be written as

$$\Delta\mathbf{x}(nT+\tau_m) = \mathbf{H}(\Omega,\ \tau_m)\mathbf{u}e^{j\Omega(nT+\tau_m)} \tag{76}$$

Substituting Eq. (76) into Eq. (75) gives

$$\begin{bmatrix} \mathbf{J}_1 & & & \mathbf{C}_1 \\ \mathbf{C}_2 & \mathbf{J}_2 & & \\ & \ddots & \ddots & \\ & & \mathbf{C}_P & \mathbf{J}_P \end{bmatrix} \cdot \begin{bmatrix} \Delta\mathbf{X}_1 \\ \Delta\mathbf{X}_2 \\ \vdots \\ \Delta\mathbf{X}_P \end{bmatrix} = \begin{bmatrix} \mathbf{u} \\ \mathbf{u} \\ \vdots \\ \mathbf{u} \end{bmatrix} \tag{77}$$

where

$$\Delta\mathbf{X}_m = \Delta\mathbf{X}(\Omega,\ \tau_m) = \mathbf{H}(\Omega,\ \tau_m)\mathbf{u}$$
$$\mathbf{J}_m = \mathbf{g}_m + \frac{\mathbf{c}_m}{h_m}, \quad \mathbf{C}_m = -e^{-j\Omega h_m}\frac{\mathbf{c}_m}{h_m}$$

The discretization step h_m is the numerical integration time step in the transient analysis for the periodic steady-state response.

Examples

The first example is the eighth-order switched capacitor bandpass filter as shown is Fig. 14. This circuit was made by cascading a third-order elliptic low-pass filter with a cutoff frequency of 3.4 kHz and a fifth-order elliptic high-pass filter with a cutoff frequency of 300 kHz. The sampling frequency is 100 kHz. First, the steady-state response is computed for the circuit with only clock excitation. Then, small signal frequency responses, that is $H_0(\omega)$, are calculated. The small signal responses of this circuit are shown in Fig. 15. The parameters in Fig. 15 are the ON resistance values. The cross marks show measured values. It is found that the high ON resistances of the switches cause attenuation in the lower stopband to deteriorate.

The second example is a direct conversion mixer circuit as shown in Fig. 16. The local oscillator signal frequency is 280 MHz with an RF signal at 280 MHz plus several kilohertz. The output frequency is several kilohertz. It is exceptionally difficult to solve the steady-state response of this circuit by

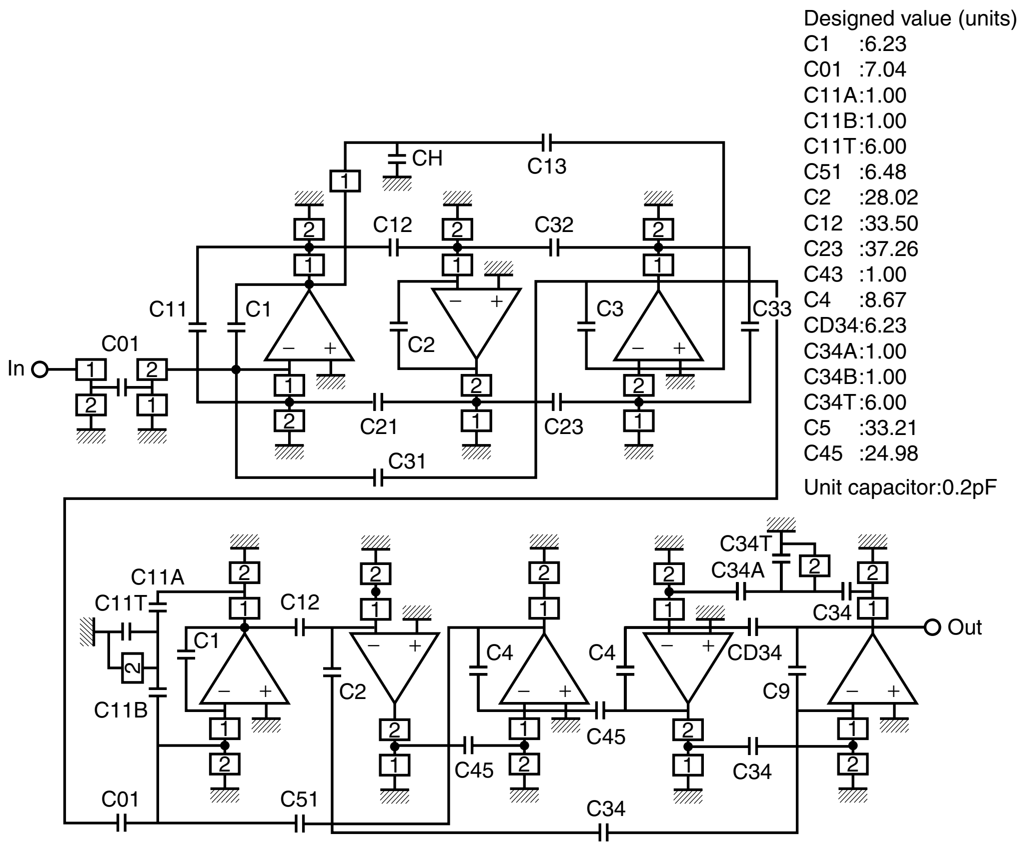

Figure 14. Eighth-order switched capacitor bandpass filter.

the conventional transient analysis because of the large difference between the output frequency and the RF and LO signal frequencies. Here, an RF input signal can be considered as a perturbation, because the circuit usually treats a small RF input. First, the periodic response with the LO signal is found. Then, the conversion gain from the RF input to the LF output, i.e., $H_{-1}(\omega)$, is computed. Figure 17 shows conversion gains and measured values for various levels of LO signal.

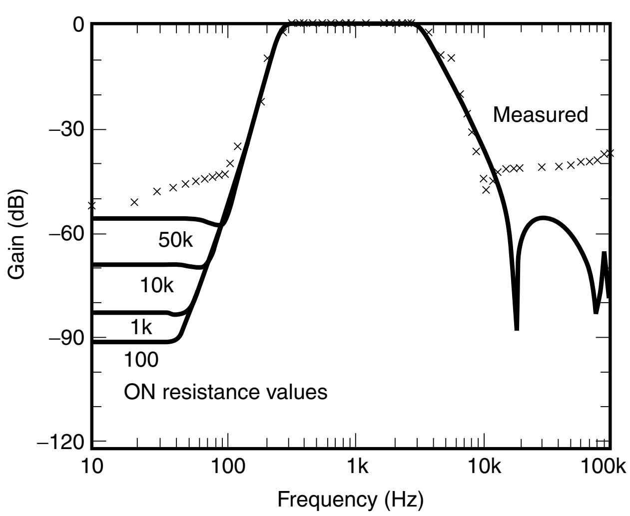

Figure 15. Small signal responses of the eighth-order SC-BPF.

NOISE ANALYSIS METHODS FOR PERIODIC NONLINEAR CIRCUITS

This section describes noise analysis methods for periodic nonlinear circuits modeled as linear periodic time-varying (LPTV) circuits, such as mixer circuits, SCFs, and oscillators.

Assuming stationary noises, the output noise spectrum density of an LPTV circuit is given by (16)

$$S(\omega) = \sum_{l=-L}^{L} |H_l(\omega - l\omega_0)|^2 \hat{s}(\omega - l\omega_0) \tag{78}$$

where $\hat{s}(\omega - l\omega_o)$ denotes a power spectral density of a certain noise source, for example, $\hat{s} = 4kTG$ for the thermal noise source of a resistor $R(G = 1/R)$. Then, the noise current source with an amplitude of $\sqrt{4kTG}$ is connected in parallel with the resistor. $H_l(\omega - l\omega_o)$ indicates a Fourier coefficient of an LPTV transfer function to the output from the noise source. The Fourier coefficients can be calculated by using the frequency-domain method (32,35) or the time-domain method (16). $H_1(\omega - \omega_o)$ denotes up-conversion from $\omega - \omega_o$ to ω and $H_{-1}(\omega + \omega_o)$ denotes down-conversion from $\omega + \omega_o$ to ω. $H_0(\omega)$ is not involved with any frequency translation. The power of each Fourier component is summed up until l value of Eq. (78) reaches L value specified by a user, or until its contribution become negligible. Figure 18 shows the noise power spectrum when the L value is 1. The total noise is calculated by summing up power spectral densities from all noise sources.

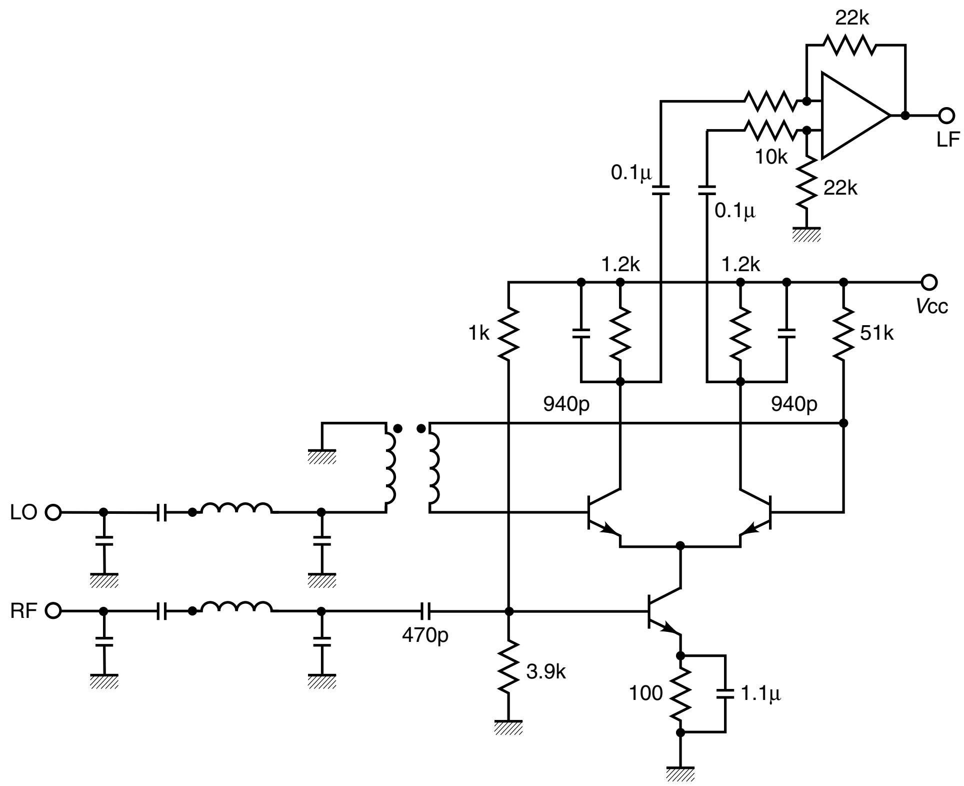

Figure 16. Direct conversion mixer circuit.

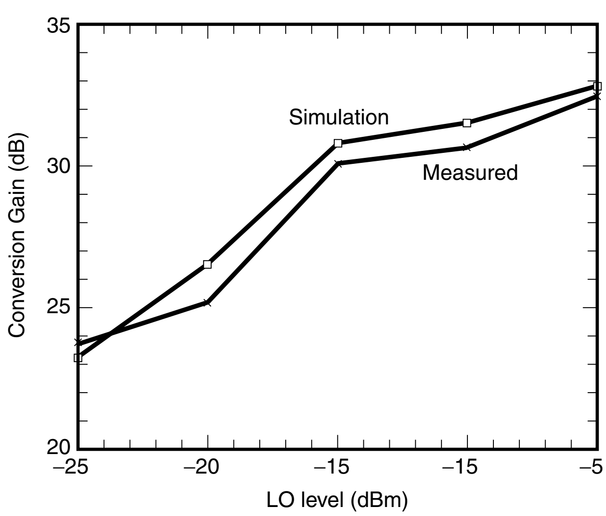

Figure 17. Conversion gain of the direct conversion mixer circuit.

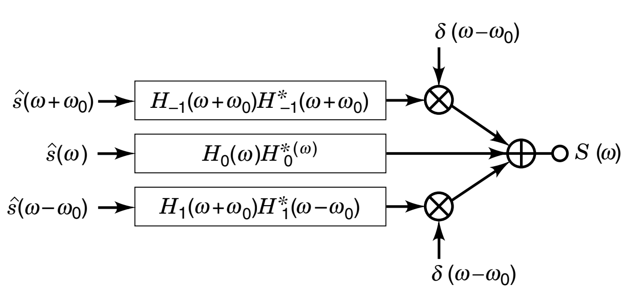

Figure 18. Noise power spectrum of LPTV circuit.

Noise analysis methods for LPTV circuits including cyclostationary noise sources have been described in previous studies (16,34). Roychowdhury (35) discusses the frequency-domain method using the harmonic balance algorithm and Okumura (16) presented a time-domain method.

Oscillator Noise

Oscillators are also periodically operating nonlinear circuits, though they have no external large excitation. The noise analysis method using the LPTV circuit model can be expanded to autonomous systems (36).

Oscillator noise simulation is an important aspect of RF circuit design. A model of oscillator phase noise spectra has been proposed by Leeson (37). This model quantitatively matches measured results. Phase and amplitude noises have been analyzed using a simple oscillator model consisting of an *RLC* resonator and a negative resistance (38). Using Kurokawa's equation (38), phase and amplitude noises have been related to the resonator's Q factor by Sweet (39). These results are important for oscillators with resonators. However, oscillators without resonators, such as ring oscillators and multivibrators, cannot be evaluated by this method. Noise simulation methods using the LPTV circuit models for oscillators with and without resonators are described in recent work (36,40,41). In these methods, periodic steady-state solutions of oscillators are calculated using the shooting method (4,5,11), or the harmonic balance method (7,10,11). Output noise spectral density of an oscillator modeled as an LPTV circuit is also shown in Eq. (78). The Fourier coefficients in Eq. (78) can be calculated by using the frequency-domain method (31) or the time-domain method (36). If you use the time-domain method, a loss-less integration method, e.g.,

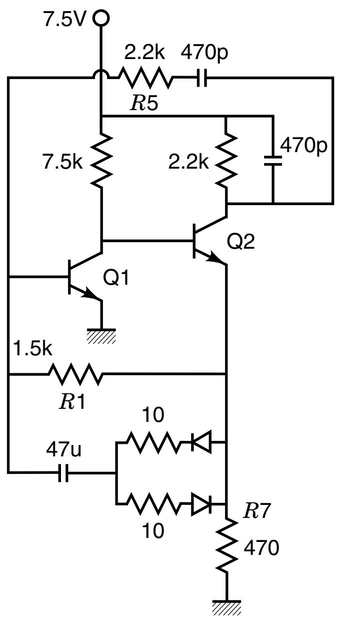

Figure 19. Wien bridge oscillator.

trapezoidal method, for numerical integration should be used for oscillator simulation (36). It is clear that we have to take into account down-converted noise as well as up-converted noise from Eq. (78). For oscillators, it is well known that up-converted flicker noise dominates near the oscillation frequency. However, it was found that down-converted noises may become dominant relative to noise near the oscillation frequency for a hard oscillation circuit, e.g., multivibrator.

The noise analysis flow is as follows.

Step 1. Compute a periodic steady-state solution.

Step 2. Store LPTV parameters during the steady-state analysis.

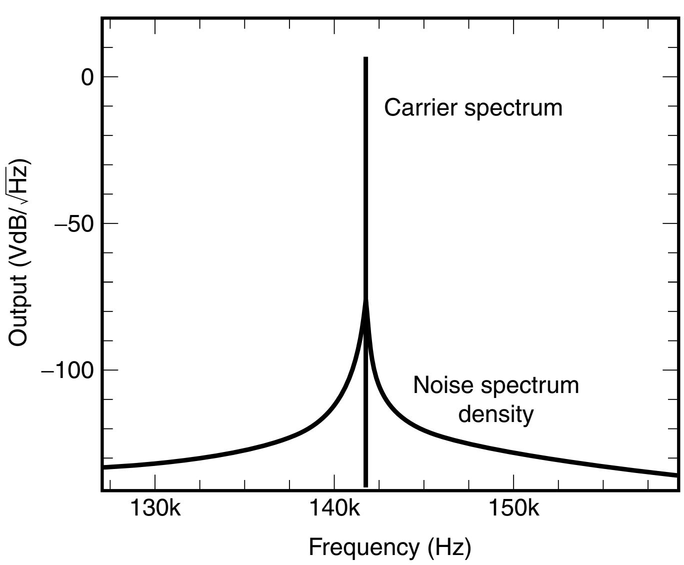

Figure 20. Noise spectral density and carrier spectrum.

Step 3. Calculate Fourier components of LPTV transfer function to the output from each noise source using the LPTV parameters.

Step 4. Accumulate Fourier components with and without frequency translation using Eq. (78).

Step 5. Compute total noise by summing up the power spectral densities calculated in *Step 4* from all noise sources.

Example

An example is a Wien bridge oscillator shown in Fig. 19. This circuit oscillates at 141.655 kHz. Figure 20 shows the noise spectral density of total noise and a line spectrum of the steady-state oscillator output. Noise sources considered are also thermal noise of resistors, shot noise, and flicker noise of transistors. Flicker noise is approximated by a stationary colored noise. The noise in this figure contains both amplitude noise and phase noise. This realizes a situation similar to that when the output is measured by a spectrum analyzer.

BIBLIOGRAPHY

1. L. O. Chua and P. M. Lin, *Computer-Aided Analysis of Electronic Circuits: Algorithms and Computational Techniques,* Englewood Cliffs, NJ: Prentice-Hall, 1975.
2. T. J. Aprille, Jr. and T. N. Trick, Steady-state analysis of nonlinear circuits with periodic input, *Proc. IEEE,* **60**: 108–114, 1972.
3. T. J. Aprille, Jr. and T. N. Trick, A computer algorithm to determine the steady-state response of nonlinear oscillators, *IEEE Trans. Circuit Theory,* **CT-19**: 354–360, 1972.
4. F. B. Grosz and T. N. Trick, Some modifications to Newton's method for the determination of the steady-state response of nonlinear oscillatory circuits, *IEEE Trans. Comput.-Aided Des.,* **CAD-1**: 116–119, 1982.
5. M. Kakizaki and T. Sugawara, A modified Newton method for the steady-state analysis, *IEEE Trans. Comput.-Aided Des.,* **CAD-4**: 662–667, 1985.
6. S. Skelboe, Computation of the periodic steady-state response of nonlinear networks by extrapolation methods, *IEEE Trans. Circuits Syst.,* **CAS-27**: 161–175, 1980.
7. K. S. Kundert, J. K. White, and A. Sagiovanni-Vincentelli, *Steady-State Methods for Simulating Analog and Microwave Circuits,* Boston: Kluwer Academic Publishers, 1990.
8. J. R. Parkhurst and L L. Ogborn, Determining the steady-state output of nonlinear oscillatory circuits using multiple shooting, *IEEE Trans. Comput.-Aided Des. Integr. Circuits Syst.,* **CAD-14**: 882–889, 1995.
9. M. Urabe, Galerkin's procedure for nonlinear periodic systems, *Arch. Ration. Mech. Anal.,* **20**: 12–152, 1965.
10. M. S. Nakhla and J. Vlach, A piecewise harmonic balance technique for determination of periodic response of nonlinear systems, *IEEE Trans. Circuits Syst.,* **CAS-23**: 85–91, 1976.
11. K. S. Kundert and A. Sangiovanni-Vincentelli, Simulation of nonlinear circuits in frequency domain, *IEEE Trans. Comput.-Aided Des. Integr. Circuits Syst.,* **CAD-5**: 521–535, 1986.
12. H. Makino and H. Asai, Relaxation-based circuit simulation techniques in the frequency domain, *IEICE Trans. Fundam.,* **E76-A**: 626–630, 1993.
13. L. O. Chua and A. Ushida, Algorithms for computing almost periodic steady-state response of nonlinear systems to multiple input frequencies, *IEEE Trans. Circuits Syst.,* **CAS-28**: 953–971, 1981.

14. C. K. Petersen, Computation of quasi-periodic solutions of forced dissipative systems, *J. Comput. Phys.,* **58**: 395–408, 1985.
15. M. Okumura, T. Sugawara, and H. Tanimoto, An efficient small signal frequency analysis method of nonlinear circuits with two frequency excitations, *IEEE Trans. Comput.-Aided Des. Integr. Circuits Syst.,* **CAD-9**: 225–235, 1990.
16. M. Okumura, H. Tanimoto, T. Itakura, and T. Sugawara, Numerical noise analysis for nonlinear circuits with a periodic large signal excitation including cyclostationary noise sources, *IEEE Trans. Circuits Syst.,* **CAS-40**: 581–590, 1993.
17. Y. Shinohara, Galerkin method for autonomous differential equations, *J. Math. Tokushima Univ.,* **15**: 53–85, 1981.
18. A. Brambilla and D. D'Amore, A filter-based technique for the harmonic balance method, *IEEE Trans. Circuits Syst. I, Fundam. Theory Appl.,* **CAS-43**: 92–98, 1996.
19. A. Ushida and L. O. Chua, Steady-state response of non-linear circuits: A frequency-domain relaxation method, *Int. J. Circuit Theor. Appl.,* **17**, 249–269, 1989.
20. T. Sugimoto, Y. Nishio, and A. Ushida, SPICE oriented steady-state analysis of large scale circuits, *IEICE Trans. Fundam.,* **E79-A**: 1530–1537, 1996.
21. A. Ushida and L. O. Chua, Frequency-domain analysis of nonlinear circuits driven by multi-tone signals, *IEEE Trans. Circuits Syst.,* **CAS-31**: 766–778, 1984.
22. K. S. Kundert, G. B. Sorkin, and A. Sangiovanni-Vincentelli, Applying harmonic balance method to almost-periodic circuits, *IEEE Trans. Microw. Theory Tech.,* **MTT-36**: 366–378, 1988.
23. A. Ushida, T. Adachi, and L. O. Chua, Steady-state analysis of nonlinear circuits based on hybrid methods, *IEEE Trans. Circuits Syst. I, Fundam. Theory Appl.,* **CAS-39**: 649–661, 1992.
24. J. J. Ebers and J. L. Moll, Large-signal behaviour of junction transistors, *Proc. IRE,* **42**: 1761–1772, 1954.
25. T. Endo and T. Ohta, Multimode oscillations in a coupled oscillator system with fifth nonlinear characteristics, *IEEE Trans. Circuits Syst.,* **CAS-27**: 277–283, 1980.
26. K. K. Clarke and D. T. Hess, *Communication Circuits: Analysis and Design,* New York: McGraw-Hill, 1969.
27. P. Wynn, Acceleration techniques for iterated vector and matrix problems, *Math. Comput.,* **10**: 301–322, 1962.
28. L. O. Chua, *Introduction to Nonlinear Network Theory,* New York: McGraw-Hill, 1969.
29. P. Penfield, Jr., Circuit theory of periodically driven nonlinear systems, *Proc. IEEE,* **54**: 266–280, 1966.
30. L. A. Zadeh, Frequency analysis of variable networks, *Proc. IRE,* **32**: 291–299, 1950.
31. V. Rizzoli, C. Cecchetti, and A. Lipparini, Frequency conversion in general nonlinear multiport devices, *IEEE MTT-S Int. Microw. Symp. Dig.,* pp. 483–486, 1986.
32. V. Rizzoli and A. Neri, State of the art and present trends in nonlinear microwave CAD techniques, *IEEE Trans. Microw. Theory Tech.,* **36**: 343–365, 1988.
33. S. A. Maas, *Nonlinear Microwave Circuits,* Dedham, MA: Artech House, 1998.
34. M. Kakizaki and T. Sugawara, An efficient numerical analysis method for small signal frequency response from periodically operating circuits, *Proc. IEEE Int. Symp. Circuits Syst.,* pp. 579–582, 1985.
35. J. S. Roychowdhury and P. Feldman, A new linear-time harmonic balance algorithm for cyclostataionary noise analysis in RF circuits, *Proc. Asia South Pac. Des. Auto. Conf.,* pp. 483–492, 1997.
36. M. Okumura and H. Tanimoto, A time-domain method for numerical noise analysis of oscillators, *Proc. Asia South Pac. Des. Auto. Conf.,* pp. 477–482, 1997.
37. D. B. Leeson, A simple model of feedback oscillator noise spectrum, *Proc. IEEE,* 329–330, 1966.
38. K. Kurokawa, Noise in synchronized oscillators, *IEEE Trans. Microw. Theory Tech.,* **MTT-16**: 234–240, 1968.
39. A. A. Sweet, A general analysis of noise in Gunn oscillators, *Proc. IEEE,* 999–1000, 1972.
40. F. X. Kaertner, Analysis of white and f^{α} noise in oscillators, *Int. J. Circuit Theory Appl.,* **18**: 485–519, 1990.
41. A. Demir and A. L. Sangiovanni-Vincenteli, Simulation and modeling of phase noise in open-loop oscillators, *Proc. IEEE Custom Integr. Circuits Conf.,* 1996.

Akio Ushida
Tokushima University
Makiko Okumura
Toshiba Corporation

PERIODIC STRUCTURES. See Slow wave structures.